ISSN: 2642-1569

International
Journal of Earth Science and Geology

Research Article

Open Access

Crystallographic and Morphological Characteristics of Natural Kaolins, Aswan Region, Egypt

A. El-Shater*, S. A. AbuSeif, A. El-Haddad and **Y. Refaey**
Geology Department, Faculty of Science, Sohag University, Egypt

Article Info

***Corresponding author:**
A. El-Shater
Geology Department
Faculty of Science, Sohag University
Egypt
E-mail: hshater@yahoo.com

Received: August 10, 2022
Accepted: October 20, 2022
Published: November 01, 2022

Citation: El-Shater A, AbuSeif SA, El-Haddad A, Refaey Y. Crystallographic and Morphological Characteristics of Natural Kaolins, Aswan Region, Egypt. *Int J Earth Sci Geol.* 2022; 4(1): 121-130.
doi: 10.18689/ijeg-1000116

Published by Madridge Publishers

Abstract

The studied area located in Aswan Governorate represents an extensive plateau bounded by irregular hills of rock units ranging in age from Pre-Cambrian to Quaternary. The kaolinite rich deposits of this area were originated from granite, mica-schist and pegmatite. These deposits were subjected to intensive laboratorial investigations (XRD, IR, EDX and SEM). These investigations indicated that kaolinite is the major clay mineral of these deposits with subordinate amounts of smectite, illite, and smectite/illite mixed layers. The non-clay minerals (e.g. quartz, feldspars, anatase and iron oxides) represent minor quantities. The coherent scattering thickness of crystallites was calculated following Scherrer, Williamson-Hall and Warren-Averbach methods using Xpowder 12 software. Additionally, the Hinckley index (HI) values of these Kaolinites were determined. The Hinckley index (HI) values of the Kaolinites weathered from pegmatite are unusual high (1.2 to 1.3 with an average of 1.25) giving conclusive evidence about the low defect nature of the clays. On contrary, the Kaolinites weathered from granites and mica-schist rocks possess considerably lower HI-values (0.87-0.97) and (0.93-1.0), respectively. The mean crystallite thickness of the studied kaolinite is varying from 22nm to 50nm. The kaolinite deposits originated from pegmatite are almost having exactly the theoretical value of the d-spacing (7.14-7.15 Å) and the best degree of crystallinity with the minimum values of strains. Based on the thickness of kaolinite crystallites, the kaolinite–rich deposits derived from mica schist had been classified as highly weathered materials. Texturally, the studied kaolinite particles are mostly classified into vermiform and fine platy types.

Keywords: Weathered profiles, Kaolinite Crystallites Morphology, HI-index, XRD-patterns

1. Introduction

Kaolinite represents one of the most significant clay minerals that occur in a considerable amount especially in sediments and sedimentary rocks (Chamley, 1989). Kaolinite usually originates from crystalline rocks as product of alteration processes. Owing to its prevalent incidence as well as its chemical and physical characteristics, kaolinite is used widely in special technical applications (e.g. ceramics, filling and refractory materials) (Murray, 2007). From sedimentary environments point of view, kaolinite considers as an essential indicator and specific mineral in sedimentary environmental conditions (Chamley, 1989).

Kaolin forms a unique large clay minerals family that is varying from perfectly ordered and defect-free minerals (Ge´ode kaolinite) to highly disordered minerals (fire clays) side by side a quasi-continuous series of intermediates in between (Tchoubar et al., 1982). The chemical as well as crystallographical diagnostics features of kaolinite are variables widely owing to its genetic nature (Fialips et. al,.1999). It was originated by weathering of parent

feldspars and micas bearing rock materials. Kaolinite deposits are usually having variable colors and properties depending upon their associated constituting components.

To assess the industrial applications of kaolinite deposits, detailed crystallographic and morphological investigations must be done and integrated with mineralogical analysis (Yvon et al., 1982; Singh and Gilkes, 1992; Melo et. al., 2001; Sei et. al., 2006). The size distributions of crystallites can be estimated using powder X-ray diffraction (XRD) due to the widths of the peaks broaden as the crystallite size decreases. The associated components usually affect the degree of disorder of clay minerals so it must be determined by adequate sample preparation (Galan et al., 1994).

Theoretically, the distribution and the shapes of crystallite thicknesses can be interpreted using Bertaut-Warren-Averbach (BWA) method based on crystal-growth mechanisms (Eberl et al., 1998). The BWA-technique has been used as a useful tool in several measurements: illite particle thickness measuring (Eberl et.al., 1998), crystallite size distribution of kaolin minerals , exploring crystal growth mechanisms for illite and smectite (Srodon et. al., 2000; Mystkowskietal., 2000), diagenetic evolution of the crystallite thickness distribution of illitic material (Kotarba and Srodon, 2000), effecting of weathering processes on smectite and illite/smectite and crystallite-size changes of pyrophyllite during grinding (Uhlik et al., 2000).

The Egyptian clayey deposits have been studied by many authors (e.g. Gad and Barrett, 1949;El-Naggar,1970; Baioumy et. al., 2012; Wageh,2017; Farouk etal.2020). However, there is scarcity of information in literature about the crystallite size of the clay minerals (including kaolinite) and the distortions of these crystallites have never been determined. So, the current study represents a part of project research (Genesis of Natural Microporous Mineral Resources and their Application in Industry) that was performed by Geology Department, Faculty of Science, Sohag University, Sohag, Egypt. This study aims to determine physicochemical, morphological and structural characteristic properties of kaolinite-rich deposits in Aswan Governorate, Egypt.

2. Geological Setting of the Study Area

The studied area locates in Aswan Governorate extending between lat. 23°30´and 24°30´ N and long. 32°30´ and 33°30´ E (Fig.1). Topographically, this area occupies an extensive plateau that bounded by irregular hills especially in its southern parts. The rock units of the studied area contain three main sequences: Pre-Cambrian, Cretaceous and Quaternary rock units. These rock units can be described briefly from older to younger as the followings:

1. Pre-Cambrian rock units

The Pre-Cambrian rock units of the studied area can be classified into:

a. Metamorphic rocks consisting of mica schist, hornblende schist, amphibolites and gneisses (Attia, 1955; Hesham, 2005).

b. Igneous rocks represented by minor intrusions, granites, granodiorite and diorites (Fig. 1).

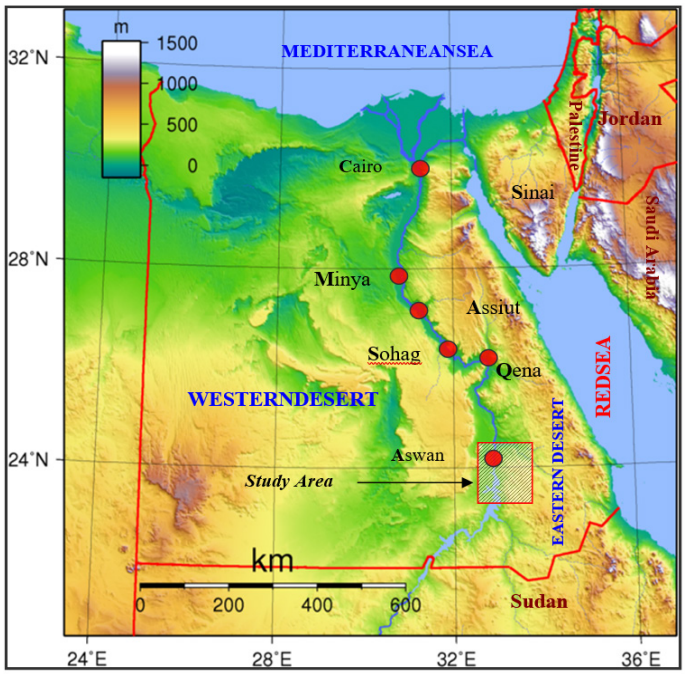

Figure 1. Location map of Aswan region and study area

2. Cretaceous rock units are disconformably overlying the Pre-Cambrian basement rocks and are representing by Nubian Group that embraces all exposed non-marine to marginal and shallow marine siliciclastics. In the study area, the Nubian Group includes three formations namely: Abu Aggag Formation, Timsah Formation and Um Baramil Formation, Salem, et. al., 2013)
   a. Um Baramil Formation
   b. Timsah Formation represented by conical hills and alternative zones of paleosol enriched in iron oxide (limonite).
   c. Abu Aggag Formation consists mainly of coarse grained bearing kaolinitie sandstone beds enriched with paleosol horizons. It has been formed under lacustrine conditions (Hussein, 1990).

3. Quaternary rock units
   a. Flood plain sediments represent the main cultivated lands in Upper Egypt that restricted to the River Nile banks.
   b. Wadi Deposits vary widely in texture and thickness based upon the land geomorphology as well as on the regime and intensity of the flash flooding events forming them.

3. Material and Methods

Detailed field investigations of the study area were done to trace the weathered materials on the Pre-Cambrian basement rocks. Nineteen representative clayey-rich samples were collected from three rock types: 9 samples from weathered deposits of granites in sites I, II and III of WadiAllaqi, 7 samples from those mica-schist in sites IV , V and VI of Wadi Abu Aggag and Wadi Abu Sobeira, and 3 samples from those of pegmatite in site VII (Table 1 and Figure. 2). These samples were subjected to several laboratory analyses: Infrared spectroscopy (IR), X-ray diffraction (XRD), Energy dispersive X-ray (EDX) and Scanning Elecron microscope (SEM).

The IR-results were interpreted based on investigation of Leitz Wetzlar spectrophotometer model III.G. The bulk samples as well as the clay-sized fractions were analyzed using XRD technique. The XRD charts were used to estimate the mineralogical composition of these rock units qualitatively and quantitatively using Xpowder12 software. Also, the size and strain of the crystallite were determined using Scherrer, Williamson-Hall, Warren-Averbach methods (Pardo et al., 2007). Additionally, the degree of structural disorder and Hinckley Index (HI) of the kaolin were evaluated using XRD-patterns of randomly oriented specimens of the clay fractions (<2 µm) according to Galan et al. (1994) and Hinckley (1963) methods, respectively.

The Decomp XR software (Lanson, 1997) was used to decompose the reflections d(001) of mica, illite and kaolinite present in clay fraction(<2µm). All diffractograms of clay fraction (<2µm, the air-dried state patterns) were submitted to decomposition assumed as diagenetic constituents to use in parameter interpretation. The width at half height and intensity of an elementary peak was used to determine its peak area which in turn was expressed as percentages of via the sum these areas (Stanjek et. al., 1992; Lanson, 1997).

Fused discs were prepared from clay-sized fraction (<2µm) to determine major oxides using a Bruker AXS S4 Pioneer XRF device (Rh-tube at 4kW), Engineering Geology, TUM University, München, Germany. Tube voltage and current for W target were 40 kV and 60 mA, respectively. Loss on ignition (LOI) was obtained by heating sample powders to 1050 °C for 6 h. The morphological and microchemical characteristics of the studied kaolinite-rich regolith samples were examined using a JOEL JSM-35C scanning electron microscope (SEM) equipped with an energy dispersive X-ray (EDX) detector (Engineering Geology, TUM University, Munich, Germany). Some specific mineral grains were isolated and analyzed using a Kevex Quantum energy-dispersive x-ray analysis unit to determine the ratios of oxides of Si, Al, K, Na, Ca, Fe, and Ti in individual minerals.

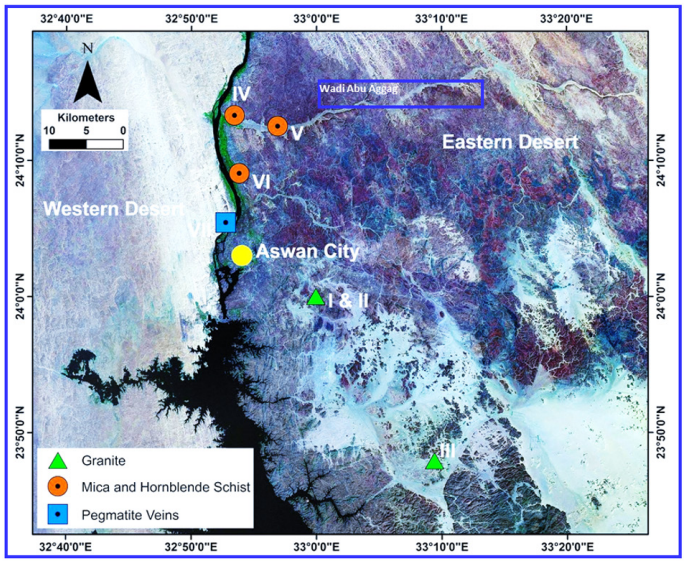

Figure 2. Landsat map of Aswan area showing the location of studied weathering profiles

Table 1. Quantification of the minerals identified by XRD of the whole rock of the studied kaolinite deposits

Sample sites	Sample No.	Phylosilicates	Quartz	Hematite	Microcline	Alunite	Anatase
Site I	1G	88.2	3	2	0	0	2.8
	2G	92.5	2.7	2.3	0	0	2.5
	3G	91.2	3	2.5	0	0	3.3
	4G	93.2	3	1.7	0	0	2.1
Site II	5G	96.5	3	0.5	0	0	0
	6G	94.6	5	0.4	0	0	0
Site III	7G	93.3	6	0.7	0	0	0
	8G	95.3	3.4	0.8	0	0	0
	9G	93.6	6	0.4	0	0	0
Site IV	10MS	90	6	0	2	0	2
	11MS	84	8.7	0	2	5	0.3
Site V	12MS	96.3	3	0.2	0	0	0.3
	13MS	91.6	4	0.2	0	0	0.2
Site VI	14MS	91.5	8	0.2	0	0	0.3
	15MS	93.6	6	0.2	0	0	0.2
	16MS	93.5	6	0	0	0	0.5
Site VII	17P	96	1	0	3	0	0
	18P	97	1	0	2	0	0
	19P	97	1	0	2	0	0
Average		93.1	4.2	0.64	0.58	0.26	0.76

4. Results and Discussion

4.1. Mineralogy of the Weathering Zones

4.1.1. IR analysis: The obtained IR-charts are characterized by four regions of vibrations. These regions are considered as conclusive evidence and diagnostic features of the kaolinite spectrum (Farmer, 1974; Olphen and Fripiat, 1979; Wilson, 1994). These regions are: O-H stretching (3700-3620 cm^{-1}), Si-O stretching (1120-1000cm^{-1}), O-H bending (940-910cm^{-1}) and the SiO_2 bending (550-400 cm^{-1}) regions (Fig 3).

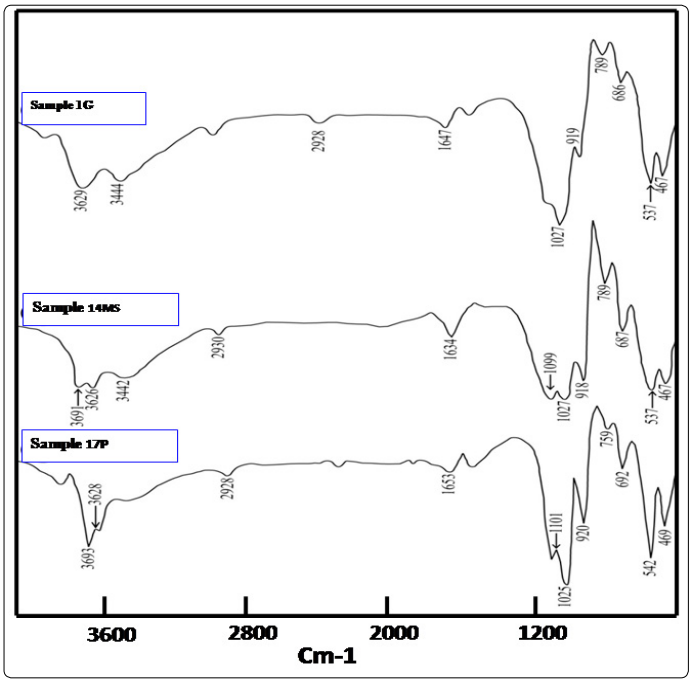

Figure 3. Represents IR-spectra of < 2µm clay fraction of the studied profiles at WadiAllaqi Road, WadiAgabat and west Aswan (1G, 14MS, 17P respectively)

Figure 3 illustrates most of the medium intensity appears as a doublet with 3670cm^{-1} band and 3652cm^{-1} band. This feature indicates increasing in crystallinity and high order of the clay crystal (Wilson, 1994). Muscovite occurs as an intense band at 3628cm^{-1} vibration (Vedder and Wilkins, 1969). Consequently, the occurrence of kaolinite and muscovite can be confirmed by presence of Si–O stretched bands locating in 1113cm^{-1} and 1040cm^{-1} region, respectively (Vedder, 1964; Kristof et.al., 1993).

The Al-Al-OH bending vibrations at 923.6cm^{-1} region give a marked indication of dioctahedricity of kaolinite and muscovite. Additionally, the bending and stretching vibrations of water hydration are manifesting at 3428.6 cm^{-1} and 1680cm^{-1} band respectively. The weak bands (ranging from 924cm^{-1} to 550cm^{-1}) are believed to be occurred as a result of octahedral and tetrahedral substitutions. While the presence of 836cm^{-1} band is owing to Al-Mg-OH vibrations (Madejova et. al., 1992). The clay minerals tetrahedral bending mode (Al-O-Si, Si-O-Mg and Si-O-Si) are usually occurred at 545cm^{-1}, 472cm^{-1} and 429cm^{-1}, respectively (Srasra et al., 1994).

4.1.2. XRD analysis: 4.1.2.1. Bulk mineralogy: The XRD patterns of the studied weathered materials (regolith) revealed that the bulk mineralogy of these materials are mainly of phyllosilicates (84-97%, with an average of 93%) with minor amounts of quartz (1-9 %), feldspars (mainly microcline 0-3%) hematite (0-3%) anatase (0-3%) andalunite (0-5%) (Table 1 and Figure 4).

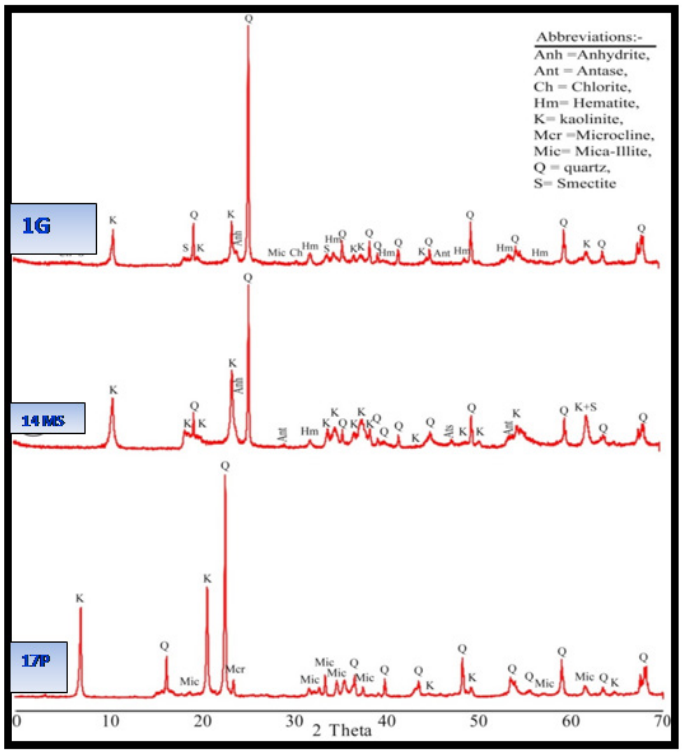

Figure 4. XRD patterns of representative bulk samples from the studied weathered granites, weathered Mica-schist and weathered pegmatites (1G, 14 MS and 17P, respectively)

4.1.2.2. Mineralogy of clay fraction (< 2µm): Kaolinite (53-97% with an average of 77%) is the principal clay mineral in The clay-sized fractions of the studied weathered materials with subordinate quantities of illite (average of 10%), smectite (average of 9%), chlorite (average of 2%) and smectite-illite mixed-layer mineral (S/I) (average of 1%). (Table 2 and Fig 5). Figure 5 shows also randomly oriented XRD patterns of (060) reflection at 1.49Å which marks a typical reflection of dioctahedralphyllosilicates enriched with kaolinite.

Table 2. Quantification of the minerals identified by XRD of the clay fraction of the studied kaolinite deposits

Sample sites	Sample No.	Kaolinite	Smectite	I-S	Mica-illite	Chlorite
Site I	1G	69	27	0	0	4
	2G	69	27	0	0	4
	3G	71	26	0	0	3
	4G	71	25	0	0	4
Site II	5G	55	9	0	36	0
	6G	53	7	0	39	0
Site III	7G	58	5	0	36	0
	8G	53	10	0	37	0
	9G	56	10	0	34	0
Site IV	10MS	83	0	12	0	5
	11MS	83	0	10	0	7
Site V	12MS	100	0	0	0	0
	13MS	92	0	0	4	4
Site VI	14MS	91	6	0	0	3
	15MS	84	12	0	0	4
	16MS	91	9	0	0	0
Site VII	17P	95	0	0	5	0
	18P	97	0	0	3	0
	19P	96	0	0	4	0
Average		77	9	1	10	2

*I-S: Illite -smectite mixed-layer mineral

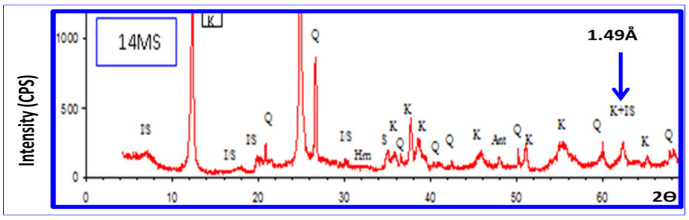

Figure 5. XRD patterns of representative non-oriented samples (<2µm) from the studied profiles (14MS, Weathered Mica-schist).

The XRD patterns (Figure. 6) of the oriented clay fraction exhibit four typical basal reflections of kaolinite: a sharp reflection (001) at 7.15Å, small one (002) at 3.57Å, a broad peak centered around 15.15Å that followed by a small reflection (003) around 5Å and the fourth one appears as a swelled glycolation of 2:1 mineral around 18.05Å. This swelled peak has been collapsed to 10 Å after heating at 550°C as an indication of a smectite-rich phase. This swelled phase indicates a poorly crystallized pure smectite with randomly smectite/illite mixed layer mineral. This observation can be proved owing to presence broadness peak at high d-spacing values of glycolated samples. The gray shale facies is regionally extensive across the study area and range in color from medium gray to dark gray. Eleven selected samples of gray shale were subjected to XRD analysis in RIMINIX laboratory in Morocco. The results show sodic and calcic bentonite that seem to be associated with high concentrations of calcite. The gray shale facies range in thickness from approximately 1.5m to 200m. (Plate 1 and Figure. 4).

4.1.2.3. Structural and morphological characterization: As above mentioned, kaolinite is considered as the most abundant clay mineral in all the studied clayey deposits (Figs 5 and 6). The morphology of d-spacing of (001) reflections of the studied samples gives conclusive information about the degree of crystallinity of the studied samples, especially about the stacking defaults along the c-axis. The basal spacing (001) reflection at 7.15Å of pure kaolin increases with decreasing crystallinity(Trunz,1976;Tchoubar et.al.,1982). The obtained results (Table 3) show that, the studied kaolinite of weathered pegmatite zones are mostly exactly the theoretical value especially in 7.14Å -7.15Å range followed by lowest degree of crystallinity of kaolinite which related to granite and mica-schist at basal spacing of 7.24Å and 7.3 Å, respectively. The shape of kaolinite peaks (001) of weathered granite and mica-schist have maximum shifted at 12.25° 2θ and 12.5° 2θ, respectively (Table 3 and Figure 5).

Table 3. Basal spacing (Å), Full width at half maximum (FWHM), Hinckley Index (HI), crystallite sizes following Scherrer, crystallite sizes and Non-Uniform Strain % of Williamson-Hall method of the samples studied.

Sample sites	Sample No.	HI	d-spacing	FWHM	ScherrerMethod	W-hall method (CDS (nm)	Non-uniform-strain (%)
Site I	1G	0.95	7.24	0.23	27	25	0.028
	2G	0.87	7.14	0.16	49	36	0.038
	3G	0.9	7.22	.260	22	17	0.00
	4G	0.89	7.16	0.24	25	26	0.122
Site II	5G	0.97	7.14	.190	30	30	0.044
	6G	0.9	7.16	,190	31	28	0.00
Site III	7G	0.87	7.16	0.18	33	29	0.00
	8G	0.9	7.16	0.20	30	27	0.00
	9G	0.89	7.16	0.22	30	25	0.00
	Average	0.9	7.17	0.21	31	27	0.029
Site IV	10MS	1.03	7.14	0.23	39	26	0.00
	11MS	0.96	7.14	0.20	44	25	0.00
Site V	12MS	0.93	7.16	0.19	32	27	0.00
	13MS	0.96	7.16	0.19	32	29	0.00
Site VI	14MS	0.93	7.3	0.34	19	14	0.00
	15MS	0.96	7.21	0.32	20	18	0.00
	16MS	0.93	7.20	0.30	21	20	0.00
	Average	0.96	7.2	0.25	30	23	0
Site VII	17P	1.24	7.09	0.16	45	34	0.005
	18P	1.23	7.08	0.16	47	36	0.072
	19P	1.3	7.09	0.16	45	33	0.023
	Average	1.25	7.09	0.16	46	34	0.023

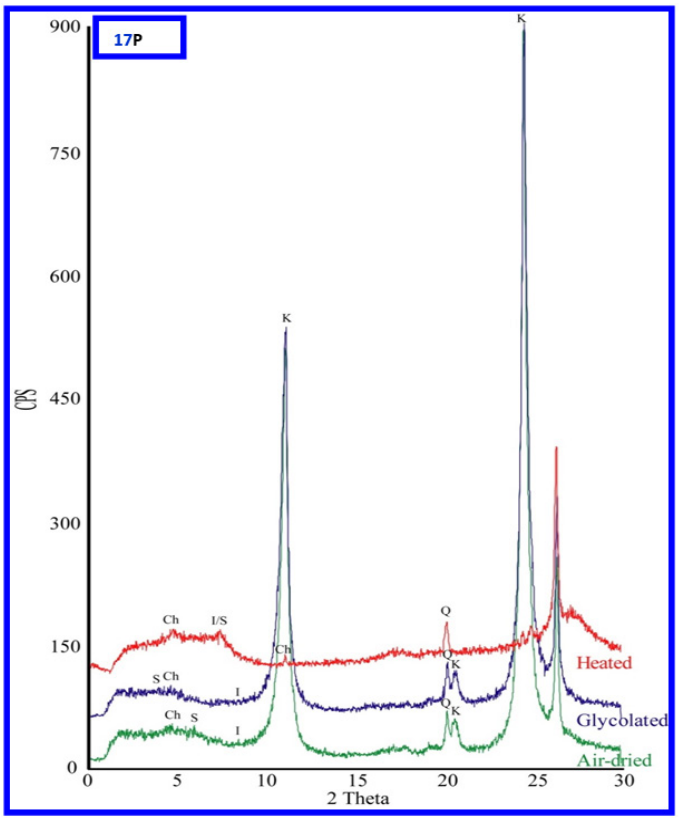

Figure 6. XRD patterns of representative oriented mount < 2mm clay fraction of the studied weathered pegmatite (K=Kaolinite; Ch= Chlorite; S=Smectite ; S/I = Smectite/Illite mixed layer mineral; I=Illite and Q=Quartz)

Kaolinite disorder was assessed using XRD peak full-widths at half maximum (FWHM) of the 7.2 Å (001) reflection and the peak intensity of the 4.45 Å (020) reflection of the <2 mm fraction in the air-dried state (Table 3). The FWHM-values is ranging from 0.16 2Ə to 0.24 2Ə with an average of 0.21 2Ə for kaolinite derived from granite, from 0.19 2Ə to 0.34 2Ə with an average of 0.25 2Ə for mica-schist rocks whereas the three samples derived from pegmatite get the same value 0.16 2Ə (Table 3).

The studied weathered pegmatites and granites kaolinite samples are showing symmetrical diffraction peaks in 12.1to 12.5 °2Ə range. Whereas, weathered mica-schists kaolinite samples are having main peaks characterized by shouldered asymmetrical diffraction especially towards the low angle diffractions (Figure 7).

The decomposition into elementary peaks of the studied kaolinite bearing deposits are illustrating that the complex peak can be explained by the sum of two elementary peaks of different equidistance, intensity and half-height width (Figure 8).

Figure 9 shows more detailed analyses of the XRD patterns of the studied samples and represents enlarged region at 19-23.5° 2θ which is illustrates a diagnostic order/disorder region of kaolinite (Noble, 1971; Aparicio and Galan, 1999; Chmielova and Weiss, 2002). In this region the 020, 110, 1$\bar{1}$1, 11$\bar{1}$ and 021 reflections of kaolinite peaks were centered near 19.7°, 20.3°, 21.2°, 21.5° and 23.0° 2θ units respectively. Additionally some reflections were observed as a centered peak near 20.75° 2θ units owing to quartz (100) reflection.

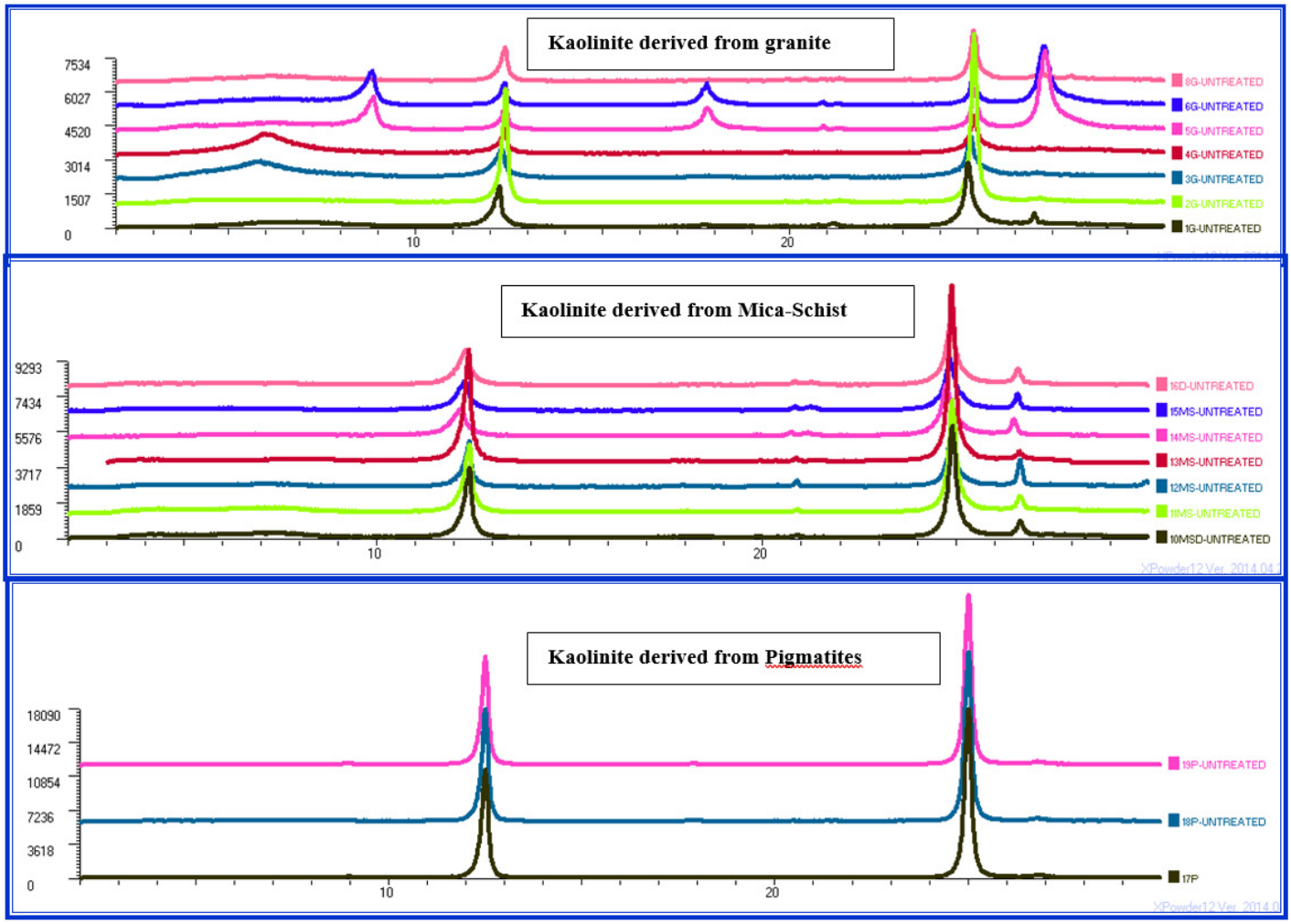

Figure 7. Comparison between XRD patterns of the studied kaolinite-rich deposits samples

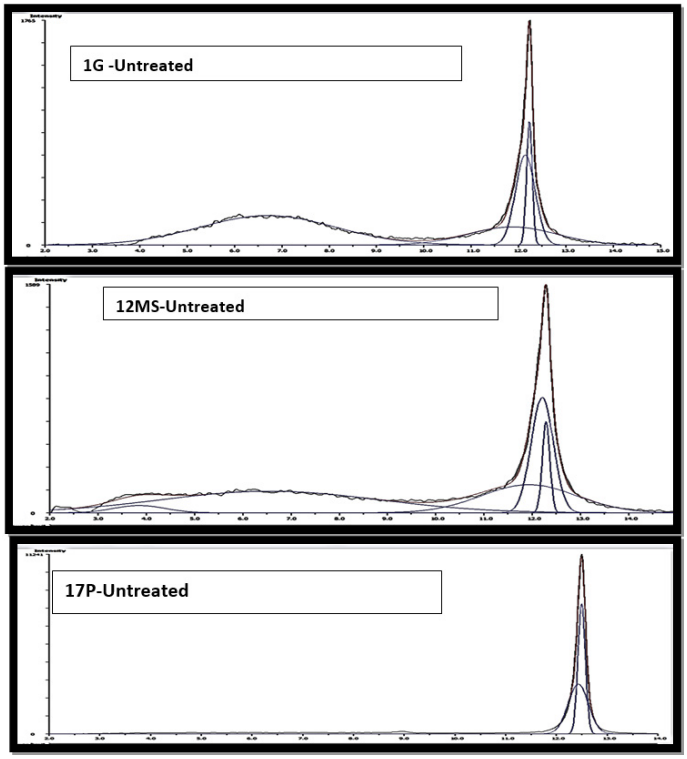

Figure 8. Decomposition of background - subtracted XRD patterns of representative samples of studied kaolinite-rich clays.

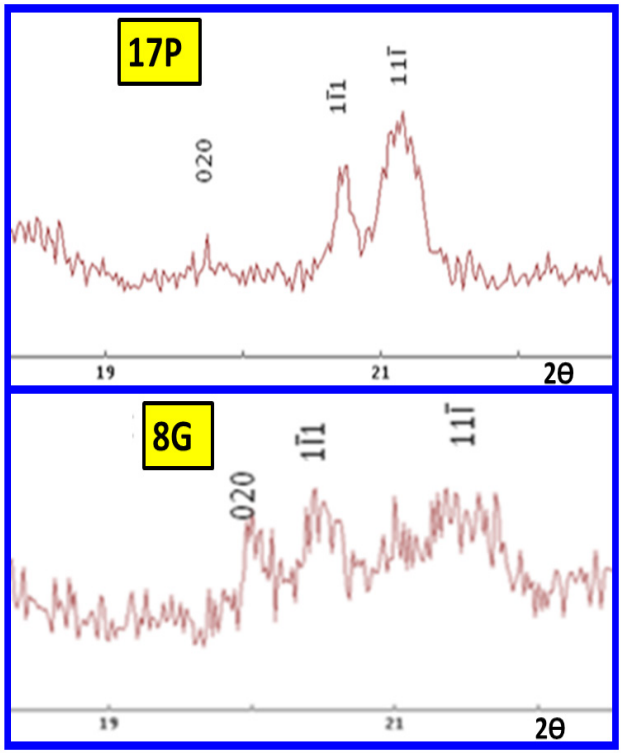

Figure 9. X-ray diffraction patterns of the studied kaolinite-rich clays in the region 19–23.5° 2θ

The reflections in above mentioned region of the XRD patterns representing the kaolinite weathered from granite and pegmatite are typically of well-ordered kaolintes (Noble, 1971; Chmielova and Weiss, 2002). On the other hand, the reflections of this region in XRD patterns of weathered mica-schist are of classically disordered kaolintes (Chmielova and Weiss, 2002; Frost et. al., 2003; Franco et al., 2004).

The intensity of the first peak with an equidistance ranging from 7.10µm to 7.14µm is attributed to pure kaolinite. Consequently, the second one of equidistance varying from 7.16 to 7.21 Å is interpreted as kaolinite crystals of lower crystallinity. The crystallinity of kaolinite is an inverse ratio to the measured equidistance and to the half-height width of the XRD peak (Brindley, 1980).

The method of Scherrer uses a single X-Ray reflection for the calculations of mosaic size, but provides no information on the 'strain' (ε), since this affects the profile differently in each 2Θvalue.The crystallite thicknesses of the studied profiles are ranging from 19to 49 nm according to the Scherrer Method (Table 3). The crystallite thicknesses of the studied samples are ranging from 17nm to 36nmand strain from 0.039 to 0.51% following the Williamson-Hall Method (Table 3). Whereas crystallite sizes obtained from Warren–Averbach method varies from 9 to 34nm and strain from 0.07 to 0.8 % (Table 4). Generally, the studied pegmatite kaolinite samples are having the highest crystallite thickness values. Additionally, the lowest strains were recorded in the kaolinite crystallites derived from pegmatites (Tables 3 and 4).

Average mean crystallite thickness of Egyptian kaolinites using the Bertaut-Warren-Averbach technique (TBWA) is slightly higher than that of selected world kaolinites (Table. 4 and Sucha et. al., 1999).

The kaolinite thickness distributions can be used as a tool to measure intensity of weathering processes. So, long and intensive weathering produces thicker kaolinite crystallites than less intensive weathering (Uhlík and Eberl, 2006). The results of the studied samples are consistent with this finding. The kaolinite–rich deposits weathered from pegmatite classified as highly weathered materials (Refaey, 2008 and Abu Seif etal.,2009)are containing thicker kaolinite crystallites than those zones weathered from granite and mica-schist rocks. The mean crystallite size obtained values of the studied samples using Warren-Averbach method are completely agree with SEM-real values of particle thicknesses (Figs.10 and 11). The range of statistical reliability of SEM-mean thickness must be up to 10nm (Srodon et al., 1992).

The kaolinite of the studied weathered pegmatite has HI-values ranging from 1.2 to 1.3 with an average of 1.25 (Table 3). These values considered as unusual higher values reflect the low defect nature of the clays. On the other hand, the kaolinite of weathered granites and mica-schist profiles are having HI-values varying from 0.87 to 0.97 and 0.93-1.0, respectively. These HI-values are considerably lower owing to lower crystallinity as well as less mature kaolin deposits than kaolinite of weathered pegmatite deposits.

4.2. Chemical Analysis:

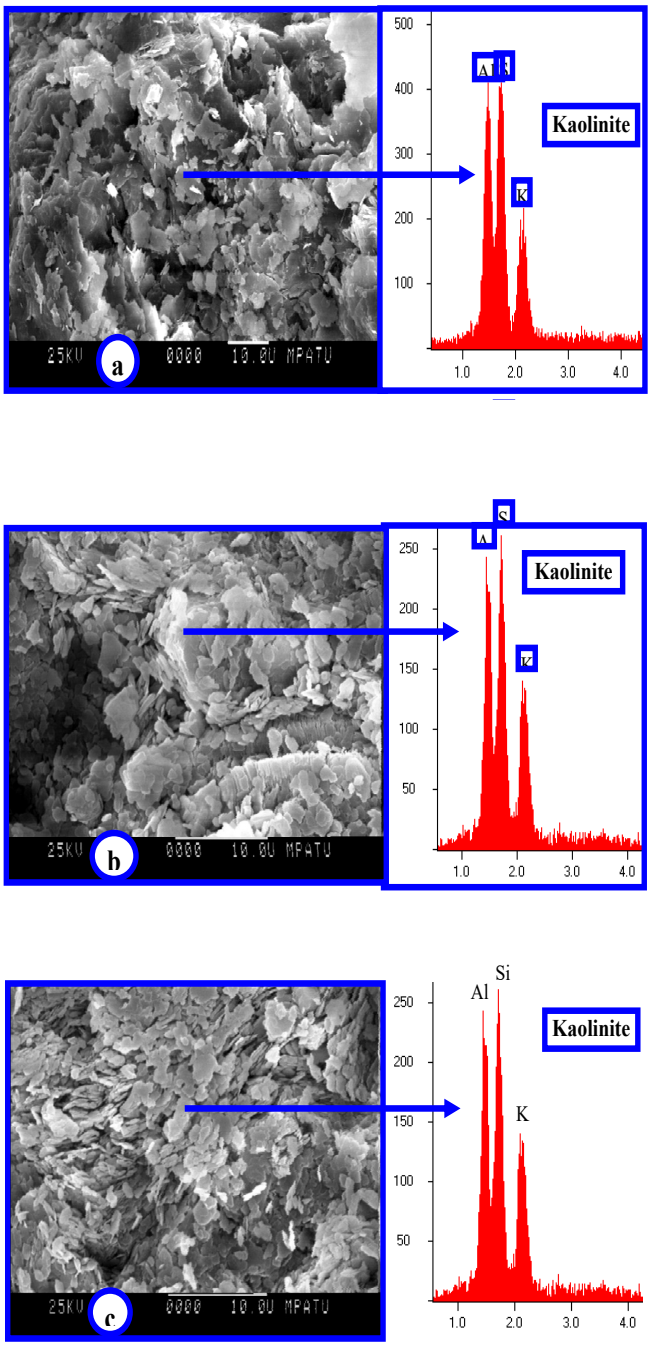

Figure 10. SEM-EDX photomicrographs of a representative samples from West Aswan showing thin, pseudohexagonal kaolinite plates

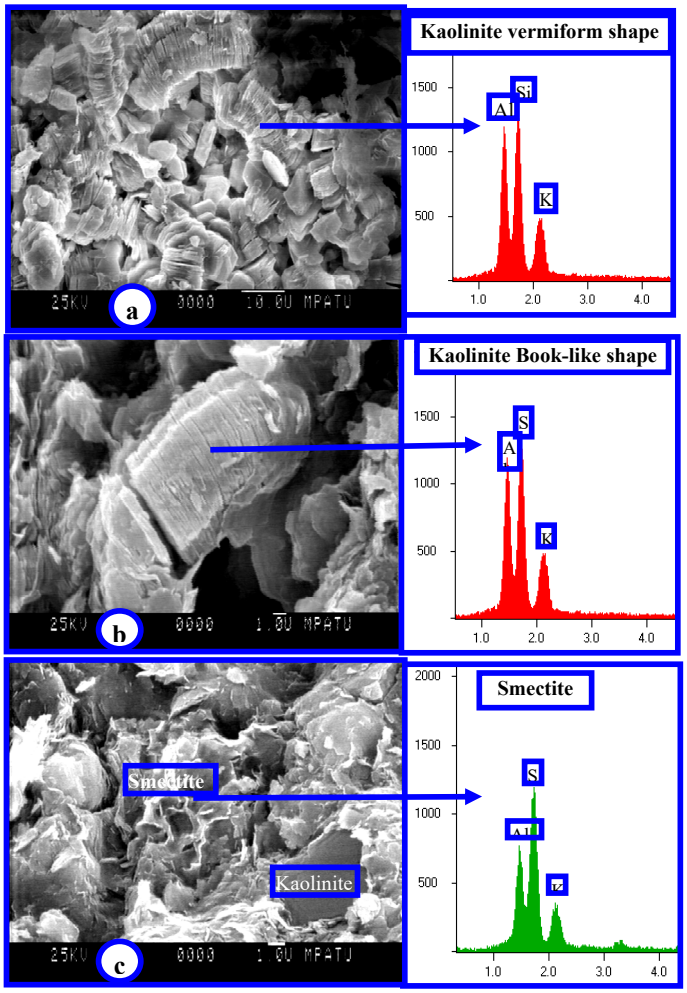

Figure 11. SEM-EDX photomicrographs of a representative samples from Wadi Abu Sobeira site VI showing booklets or stacksand vermi-form shape of kaolinite (a, b) and honeycomb texture of the smectite-rich illite (c).

It was well known that, kaolinite ($Si_2Al_2O_5(OH)_4$ must be contain 46.55 wt.% (SiO_2), 39.49 wt.% (Al_2O_3), and 13.96 wt.% (H_2O) by weight (Al-Momani etal.,2020). The qualitatively X-ray fluorescence chemical analyses of the studied samples results are mostly , revealing dominance Si and Al elements with small amounts of Fe, Ti, K, P, Mn, Ca and Mg. It was found that, the SiO_2 contents are varied greatly within the studied samples (Table 5). The obtained (SiO_2) value is being around (65%) that considered as slightly higher than the theoretical value. This is probably owing to presence of quartz and silicate minerals detected by X-ray diffraction.

The highest percentages of iron-oxides (Fe_2O_3) 10% and 20% were recorded in pegmatite and mica schist regoliths (samples 17P and 13MS). Whereas, the lower percentages (~0.4%) were observed in most of granite regolith samples (2G, 3G, 4G, 7G, 8G) and one sample of mica-schist regolith (18P) (Table 5).

From theoretical approach point of view, the pegmatite and mica-schist weathered zones attain the larger content (27-30%) of aluminum (Al_2O_3) but the lower aluminum (Al_2O_3) percentage 13- 14 % were recorded in two granite regolith samples(1G and 6G). The kaolinite rich deposits weathered from granites are particularly richer in potassium (K_2O) content (3-5 %).This may probably due to the relatively large mica (illite) content (samples 1G, 5G, 6G, Table. 4). Additionally, the kaolinite rich deposits which originated from mica-schist rocks had large amount of titanium (TiO_2) (~2%, Table 5) owing to presence of anatase detected by X-ray diffraction. The structural titanium can interpreted as result of aluminum substitution in kaolinite (Jepson and Rowse, 1975).

Table 5. Major elements and LOI concentrations of representative whole rock samples of the studied samples

Site	Sample No.	Elements (wt.%)										Loss on ignition (LOI)
		SiO_2	TiO_2	Al_2O_3	Fe_2O_3	MnO	MgO	CaO	Na_2O	K_2O	P_2O	
Site I	1G	75	0.17	12.92	1.01	0.02	0.29	0.74	3.79	4.89	0.06	0.74
	2G	79.53	0.18	13.8	0.44	0.01	0.2	0.34	0.11	0.75	0.03	5.46
	3G	78.6	0.17	14.43	0.43	0.01	0.28	0.25	0.09	1.37	0.03	4.87
	4G	74.9	0.19	16.9	0.39	0.07	0.21	0.17	0.12	1.47	0.02	5.95
Site II	5G	62.99	0.21	13.09	1.73	0.09	0.86	8.59	0.35	2.83	0.07	8.64
	6G	66.86	0.17	12.95	0.89	0.04	0.71	7.79	0.58	2.93	0.04	5.96
Site III	7G	71.6	0.19	19.9	0.26	0.07	0.26	0.17	0.18	1.49	0.08	5.8
	8G	68.6	0.21	23.6	0.3	0.07	0.21	0.14	0.16	1.29	0.02	5.4
	9G	64.6	0.21	26.7	0.3	0.07	0.21	0.21	0.13	1.25	0.02	6.3
Site IV	10MS	60.22	1.66	22.21	5.46	0.05	1.03	0.19	0.24	1.01	0.1	8.04
	11MS	69.47	1.16	17.9	0.89	0.05	0.2	0.41	0.18	0.34	0.66	8.68
Site V	12MS	51.83	1.54	29.47	5.18	0.02	0.31	0.19	0.1	0.11	0.29	11.05
	13MS	56.47	1.34	14.4	19.53	0.13	0.29	0.13	0.09	0.28	0.32	6.35
Site VI	14MS	56.51	1.47	22.52	8.15	0.36	1.04	0.18	0.33	0.43	0.09	9.14
	15MS	56.97	1.43	24.31	5.87	0.01	0.89	0.41	0.14	0.58	0.06	9.51
	16MS	56.77	1.52	27.06	3.53	0.01	0.51	0.23	0.15	0.27	0.06	10.21
Site VII	17P	54.89	1.2	21.72	10.09	0.02	2.06	0.2	0.42	1.4	0.06	8.18
	18P	79.38	0.05	14.1	0.37	0.05	0.37	0.06	0.11	0.66	0.03	5.07
	19P	65.59	0.47	23.21	0.97	0	0.29	0.11	0.14	1.66	0.04	7.93

4.3. SEM Results

Usually each clay mineral species is exhibiting various particle shapes according its integrated genetic conditions of crystallization (e.g. crystallization duration, medium pH, temperature and chemical composition of original parent rock). The crystallization duration, particle size and grain shape of these clay mineral species are mostly not independent. The size and shape variation of the kaolin subgroup crystals is so great diagnostic characteristics but cannot be used alone to distinguish kaolin subgroup from other clay mineral groups (Kanket etal.2005). Consequently, the presence of one or more 120° angles on the edge of plate can still be used as reasonable evidence of kaolinite. The variation in thickness of kaolinite flakes caused the variation in color from dark grey with thick flakes to light grey with thin flake.

Based on SEM-images, the studied kaolinite particles can be texturally classified into two types: vermiform or book-like of kaolinite aggregates and fine platy kaolinite crystals with subhedral to euhedral pseudohexagonal grains (<5 µm of diameter) arranged randomly with feldspars grains.

The vermiforms (books) are worm-shaped crystal masses consisting mainly of stack-like platy crystals with bends and undulations of the parallel slides (Meunier, 2005). Morphologically, the kaolinite grains of thinly pseudohexagonal plates are commonly observed in clay-sized weathered materials as well as in all coarser fractions. The pseudohexagonal grains are usually well observed owing to 120° angles, but the hexagonal symmetrical shapes are not present in the crystal structure.

The SEM-EDX investigations of the studied regoliths are confirming that, feldspars (Plagioclase feldspar, K-feldspar), biotite and muscovite representing the main primary minerals. The obtained EDX-data indicating that, kaolinite contains nearly the same amounts of Al and Si with minor amount of K. Similarly, illite (mica) and etched feldspar (orthoclase or plagioclase) are principally containing (K, Al, and Si) and (Si, Al, K, and Ca), respectively. Fe, Al, Si, Mg and K were represented as a thin layer coating kaolinite crystals owing to alteration of biotite and iron oxides (e.g. goethite and hematite).

Both EDX and XRD analyses indicate that the main secondary minerals of the studied samples are mainly of kaolinite, illite, allunite and smectitic minerals. Smectite was recorded in the studied sample XRD-patterns as well as it had been observed within SEM-images but with minor amount.

5. Summary and Conclusions

- Kaolinite is the major clay mineral of these weathered deposits with minor amounts of smectite, illite, and smectite/illite mixed layers. The non-clay minerals (e.g. quartz, feldspars, anatase and iron oxides) occur in trace quantities.
- The obtained IR-charts are characterized by four regions (3700-3620 cm-1, 1120-1000cm-1, 940-910cm-1 and 550-400 cm-1) of vibrations and diagnostic features of the kaolinite spectrum.IR charts and XRD patterns of the studied samples indicated the dioctahedricity of kaolinite.
- The studied kaolinite deposits that originated from pegmatite possess almost exactly the theoretical value of the d-spacing (7.14-7.15A°) and the best degree of crystallinity whereas kaolinite deposits of weathered granite mica-schist rocks are the least degree of crystallinity (7.24A°).
- Based on kaolinite crystallites thickness, the kaolinite related to pegmatiteand granite are typical of well-ordered ones, while the kaolinite of mica-schist are typical of disordered.
- The mean crystallite size obtained values of the studied samples using Warren-Averbach method are completely agree with SEM-real values of particle thicknesses.
- The kaolinites derived from pegmatites attain the lowest strain percentage following the Methods of Warren-Averbach and Williamson-Hall.
- The Hinckley index (HI) values of weathered pegmatite kaolinite are higher than those of weathered granite and mica-schist kaolinite.
- The average TBWA of the Egyptian kaolinites is slightly higher than the TBWA of selected world kaolinite
- Texturally, the studied kaolinite particles are mostly classified into two: vermiform or book-like of kaolinite aggregates.

Acknowledgment: We wish to thank Mrs. Katharina and Mr. JuergenFroh, technicians of clay and X-ray diffraction laboratory and Electron Microscope unites at TUM University, Munich, Germany for their assistance. Special gratitude goes to all the members in the Geology Department, Sohag University. They have always been friendly and helpful in the work.

References

1. AbuSeif ESA, El-Shater A, El-Haddad A, Refaey Y. Mineralogical and Geotechnical studies on the weathered zones of the basement rocks of Aswan Area, Egypt. 6th international conference on the geology of Africa, Assiut University, Egypt. 2009.
2. Al-Momani T, Alqudah M, Dwairi M. Mineralogical and Geochemical Characterization of JarashKaolinitic Clay, Northern Jordan. Jordan. *Journal of Earth and Environmental Sciences*. 2020; 11(4): 272-281.
3. Aparicio P, Galan E. Mineralogical interference on kaolinite crystallinity index measurements. *Clay and Clay Minerals*. 1999; 47(1): 12-27. doi: 10.1346/CCMN.1999.0470102
4. Attia MI. Topography, Geology and Iron Ore Deposits of East Aswan: Geol Survey Egypt, Cairo. 262 pp. 1955.
5. Baioumy HM, Gilg HA, Taubald H. Mineralogy and geochemistry of the sedimentary kaolin deposits from sinai, egypt: implications for control by the source rocks. *Clays and Clay Minerals*. 2012; 60(6): 633-654.
6. Brindley GW. Order-disorder in clay mineral structures. Mineralogical Soc London. 495. 1980.
7. Chamley H. Clay Sedimentology. Springer-Verlag, Berlin. 1989.
8. Chmielova M, Weiss Z. Determination of structural disorder degree using an XRD profile fitting procedure: Application to Czech kaolins. *Appl Clay Sci*. 2002; 22, 65-74. doi: 10.1016/S0169-1317(02)00114-X
9. Farmer VC. The Layer Silicates. Mineralogical Society, London. 331-363. 1974.

10. Fialips CI, Petit S, Decarreau A. Influence du pH, du mate´riaude de´partet de la dure´e de synthe`sesur la cristallinite´ de la kaolinite. *Comptes Rendu Acade´mie des Sciences, Paris*. 1999; 328: 515-520. doi: 10.1016/S1251-8050(99)80132-3

11. Eberl DD, Drits V, Srodon, J. Deducing growth mechanisms for minerals from the shapes of crystal size distributions. *Am J Sci*. 1998; 298, 499-533.

12. Eberl DD, Nuesch R, Sucha V, Tsipursky S. Measurement of found mnentalillite particle thickness by X-ray diffraction using PVP-10 intercalation. *Clays and Clay Min*. 1998; 46: 89-97. doi: 10.1346/CCMN.1998.0460110

13. El-Naggar ZR. On a proposed lithostratigraphic subdivision of the late Cretaceous-Early Paleogene succession in the Nile Valley, Egypt. UAR 7th Arab Petrol Congr, Kuwait. 1970; 64(B-3): 1-50.

14. Farouk S, El-Desoky H, Heikal M, El-Mahallawy M, Wahid A. Egyptian Cretaceous clay deposits: Insights on Mineralogy, Geochemistry, and Industrial uses. *Arabian Journal of Geosciences*. 2020; 13: 556. doi: 10.1007/s12517-020-05557-7

15. Franco F, Pérez-Maqueda LA, Pérez Rodriguez JL. The effect of ultrasound on the particle size and structural disorder of a well-ordered kaolinite. *J Colloid Interface Sci*. 2004; 274: 107-117. doi: 10.1016/j.jcis.2003.12.003

16. Frost RL, Kristof J, Mako E, Horvat E. A DRIFT spectroscopic study of potassium acetate intercalated mechanochemically activated kaolinite. *Spectrochim Acta Part A*. 2003; 59: 1183-1194.

17. Gad GM, Barrett LR. The constitution of some Egyptian clays. *Mineralogy Magazine*. 1949; 28(205): 587-597.

18. Galan E, Aparicio P, Gonzales I, Laiglesia A. Influence of associated components of kaolin on the degree of disorder of kaolinite as determined by XRD. *Geologica Carpathica Clays*. 1994; 45: 59-75.

19. Jepson WB, Rowse JB. The composition of kaolinite-An electron microscope microprobe study. 1975; *Clays and Clay Minerals*. 23: 310-317.

20. Hesham AA. A study of the Aswan archeological quarries, rates of weathering and deterioration of granites and the technology of petrifying in ancient Egyptians. South Valley University, Egypt. 230. 2005.

21. Hinckley DN. Variability in crystallinity values among kaolin deposits of the coastal plain of Georgia and South Carolina. *Clays and Clay Min*. 1963; 11: 229-235. doi: 10.1346/CCMN.1962.0110122

22. Hussein AA. Mineral deposits of Egypt. In: Said, R. (Ed.), Geology of Egypt. Bakema Publ. Co. Amsterdam. 733pp. 1990.

23. Kanket W, Suddhiprakarn A, Kheoruenromne I, Gilkes RJ. Chemical and crystallographic properties of kaolin from ultisols in Thailand. *Clays and Clay Minerals*. 2005; 53(5): 478-489. doi: 10.1346/CCMN.2005.0530505

24. Kotarba M, Srodon J. Diagenetic evolution of crystallite thickness distribution of illitic material in Carpathian shales, studied by the Bertaut-Warren-Averbach XRD method (MudMaster computer program). *Clay minerals*. 2000; 35: 383-391. doi: 10.1180/000985500546855

25. Kristof E, Zoltan AJ, Vassanyj I. The effect of mechanical treatment on the crystal structure and thermal behavior of kaolinite. *Clays and Clay Minerals*. 1993; 415: 608-612.

26. Lanson B. Decomposition of experimental X-ray diffraction patterns Žprofile fitting: a convenient way to study clay minerals. *Clays and Clay Minerals*. 1997; 45: 132-146

27. Madejova J, Putyera K, Cicel B. Proportion of central atoms in octahedral layers of smectites calculated from IR spectra. *Geologica Carpathica Series Clays*. 1992; 43: 117-120.

28. Melo VF, Singh B, Schaefer CEGR, Novais RF, Fontes MPF. Chemical and Mineralogical Properties of Kaolinite-Rich Brazilian Soils. *SSSAJ*. 2001; 65(4): 1324-1333. doi: 10.2136/sssaj2001.6541324x

29. Meunier A. Crystal structure of clay minerals. Clays book, ISBN 3-540 21667-7. Springer Berlin Heidelberge New York. 465. 2005.

30. Murray HH. Applied Clay Mineralogy: Occurrences, Processing and Applications of Kaolins, Bentonites, Palygorskite-Sepiolite, and Common Clays. *Developments in Clay Science*. 2007; 2: 180.

31. Mystkowski K, Srodon J, Elsass F. Mean thickness and thickness distribution of smectite crystallites. *Clay Minerals*. 2000; 35: 545-557. doi: 10.1180/000985500547016

32. Noble FR. A study of disorder in kaolinite. *Clay Miner*. 1971; 9: 71-80.

33. Pardo P, Bastida J, Kojdecki MA, Ibáñez R, Zbik M. X-ray diffraction line broadening in dry grinding of kaolinite. *Z Kristallogr Suppl*. 2007; 26, 549-554.

34. Olphen VH, Fripiat JJ. Data handbook for clay minerals and other non metallic materials. Pergamon Press, Oxford. 346. 1979.

35. Refaey YM. Mineralogical and geotechnical studies on the weathered zones of the basement rocks of Aswan area, Egypt. M.Sc. Thesis, Fac of Science Geol Dep, Sohag Univ. Egypt. 239. 2008.

36. Salem SM, El Gammal EA, Soliman NM. Morphostructural record of iron deposits in paleosols, cretaceous Nubian Sandstone of Lake Naser basin, Egypt, Western Desert, Egypt. *The Egyptian Journal of Remote Sensing and Space Sciences*. 2013; 16, 71-82.

37. Sei J, Morato F, Kra G, Staunton S, Quiquampoix H, Jumas JC, Olivier-Fourcade J. Mineralogical, crystallographic and morphological characteristics of natural kaolins from the Ivory Coast (West Africa). *Journal of African Earth Sciences*. 2006; 46: 245-252.

38. Singh B, Gilkes RJ. Properties and distribution of iron oxides and their association with minor elements in the soils of south-western Australia. *Journal of Soil Science*. 2006; 43(1): 77-98.

39. Srodon J, Elsass F, McHardy WJ, Morgon DJ. Chemistry of illite-smectite inferred from TEM measurements of fundamental particles. *Clay Minerals*. 1992; 27: 137-158.

40. Środoń J, EberL DD, Drits V. Evolution of fundamental particle size during illitization of smectite and implications for reactions mechanism. *Clays and Clay Minerals*. 2000; 48, 446-458. doi: 10.1346/CCMN.2000.0480405

41. Srasra E, Bergaya F, Fripiat JJ. Infrared spectroscopy study of tetrahedral and octahedral substitutions in an interstratified illite-smectite clay. *Clays and Clay Miner*. 1994; 43: 237-241.

42. Stanjek H, Niederbudde EA, Hfiusler W. Improved evaluation of layer charge of n-alkylammonium treated fine soil clays by Lorentz- and polarization-correction and curve fitting. *Clay Miner*. 1992; 27: 3-19. doi: 10.1180/claymin.1992.027.1.02

43. Sucha V, Kraus I. Samajova E, Puskelova L. Crystallite size distribution of kaolin minerals. *Per Mineral*. 1999; 68(1): 81-92.

44. Trunz V. Influence of crystallite on the apparent basal spacings of kaolinite. *Clays and Clay Minerals*. 1976; 24: 84-87. doi: 10.1346/CCMN.1976.0240206

45. Vedder W. Correlations between infrared spectrum and chemical composition of mica. *Am Mineral*. 1964; 49: 736-768.

46. Vedder W, Wilkins RWT. Dehydroxylation and rehydroxylation, oxidation and reduction of micas. *American Mineralogist*. 1969; 54: 482-509.

47. Wageh M. The Nature, Origin and Distribution of Kaolinite in the Lower Paleozoic Naqus Formation along Western Side of Gulf of Suez, Egypt. *Journal of Nature and Science*. 2017; 15: 49-61.

48. Wilson MJ. Clay Mineralogy: Spectroscopic and Chemical Determinative Methods. Chapman and Hall, London. (Chapter 3). 1994.

49. Uhlik P, Ucha V, Eberl DD, Pukelova L, APlovicova M. Evolution of pyrophyllite particle sizes during dry grinding. *Clay Minerals*. 2000; 35: 423-432. doi:10.1180/000985500546774

50. Uhlík P, Eberl DD. Evaluation of powder XRD data using the Mudmaster and Rockjock computer programs. *Acta Mineralogica-Petrographica*. 2006; Abstract Series 5.

51. Yvon J, Garin P, Delon JF, Cases JM. Valorisation des argiles kaoliniques des Charentes dans le caoutchouc naturel. *Bulletin de Mineralogie*. 1982; 105: 535-541.